





Structural, magnetic, and magnetocaloric properties of Fe₇Se₈ single crystals

Cite as: J. Appl. Phys. **124**, 143902 (2018); <https://doi.org/10.1063/1.5042344>

Submitted: 31 May 2018 . Accepted: 17 September 2018 . Published Online: 11 October 2018

I. Radelytskyi , P. Aleshkevych , D. J. Gawryluk, M. Berkowski, T. Zajarniuk , A. Szewczyk, M. Gutowska, L. Hawelek, P. Włodarczyk, J. Fink-Finowicki, R. Minikayev, R. Diduszko, Y. Konopelnik, M. Kozłowski, R. Puzniak , and H. Szymczak



View Online



Export Citation



CrossMark

ARTICLES YOU MAY BE INTERESTED IN

Low-field magnetocaloric effect in single crystals controlled by magnetocrystalline anisotropy
Applied Physics Letters **113**, 133902 (2018); <https://doi.org/10.1063/1.5052412>

On entropy determination from magnetic and calorimetric experiments in conventional giant magnetocaloric materials

Journal of Applied Physics **123**, 145101 (2018); <https://doi.org/10.1063/1.5016858>

Magnetoresistance, magnetic, and dielectric properties of LuFe₂O₄ prepared by ebeam-assisted solid state reaction

Journal of Applied Physics **124**, 144101 (2018); <https://doi.org/10.1063/1.5042514>

Applied Physics Reviews
Now accepting original research

2017 Journal
Impact Factor:
12.894



Structural, magnetic, and magnetocaloric properties of Fe₇Se₈ single crystals

I. Radelytskyi,^{1,2} P. Aleshkevych,¹ D. J. Gawryluk,^{1,3} M. Berkowski,¹ T. Zajarniuk,¹
 A. Szewczyk,¹ M. Gutowska,¹ L. Hawelek,⁴ P. Włodarczyk,⁴ J. Fink-Finowicki,¹
 R. Minikayev,¹ R. Diduszko,^{1,5} Y. Konopelnik,¹ M. Kozłowski,^{1,5} R. Puźniak,¹
 and H. Szymczak¹

¹*Institute of Physics, Polish Academy of Sciences, Aleja Lotników 32/46, PL-02668 Warsaw, Poland*

²*Jülich Centre for Neutron Science (JCNS) at MLZ, Forschungszentrum Jülich GmbH, Garching, Germany*

³*Laboratory for Multiscale Materials Experiments, Paul Scherrer Institut, CH-5232 Villigen PSI, Switzerland*

⁴*Institute of Non-Ferrous Metals, J. Sowinskiego 5, PL-44100 Gliwice, Poland*

⁵*Tele and Radio Research Institute, Ratuszowa 11, PL-03450 Warsaw, Poland*

(Received 31 May 2018; accepted 17 September 2018; published online 11 October 2018)

The magnetocaloric effect has been studied in high quality single crystals of Fe₇Se₈ (3c type) grown by using Bridgman's method. Magnetization and magnetocaloric effect measurements have been carried out in a magnetic field up to 5 T over the temperature range from 2 to 490 K. The spin reorientation transition from the easy *c*-axis to the easy *c*-plane, proceeding in an abrupt fashion, as a first-order phase transition, has been observed near the temperature $T_R \approx 125$ K. The magnetization curves in the vicinity of this transition were shown to have an S-shape with a clear hysteresis. The first order metamagnetic field induced transitions have been identified above and below T_R . The conventional magnetocaloric effect related to the metamagnetic transitions has been found above T_R , while below T_R the inverse magnetocaloric effect was clearly seen. The existence of both kinds of magnetocaloric effect is important from the point of view of large rotating field entropy change in Fe₇Se₈ single crystals. The refrigeration capacity associated with a second order phase transition from the ferrimagnetic to the paramagnetic state at the Néel temperature $T_N \approx 450$ K was found to be weaker than that appearing near T_R . The giant anisotropy of the magnetocaloric effect was related to the magnetic anisotropy of Fe₇Se₈ crystals. The one-ion model of the magnetocaloric effect has been developed and its predictions have been compared with experimental data. Published by AIP Publishing. <https://doi.org/10.1063/1.5042344>

I. INTRODUCTION

Iron-chalcogenides have recently attracted great interest due to the unexpected discovery of superconductivity in FeSe-based compounds.¹ Among these superconductors, FeSe has the simplest crystal structure composed of single conducting planes. Such a layered structure exhibits various magnetic interactions within layers and across a set of layers. A long range magnetic ordering is observed in nonstoichiometric Fe₇Se₈ alloys. This material has been studied for a long time.^{2–10} It has a NiAs-like structure. The iron deficiency in Fe₇Se₈ results in the appearance of vacancies at the cation sites. The Fe vacancies are usually ordered and the superstructures related to the distribution of these vacancies strongly depend on the synthesis method. Fe₇Se₈ can be formed mainly in two superstructures. For samples cooled to room temperature in the furnace, the 4c structure is realized with the unit cell four times larger along the *c*-axis than that of the fundamental NiAs-type cell. Quenching from the high temperature region leads to the appearance of the 3c structure with the *c* lattice constant three times larger than that of NiAs (see Ref. 2 and references therein). In both systems, the metal-full and metal-deficient layers are alternatively stacked along the *c* direction. A magnetic order in the alloy is a direct consequence of the existence of vacancies. Neutron diffraction measurements³ have shown that the Fe moments are arranged parallel in the same layer but they are antiparallel to the moments in the adjacent layer, leading to the

ferrimagnetic behavior of Fe₇Se₈^{4–6} with the Néel temperature $T_N = 455$ K.³ The easy axis of Fe₇Se₈ lies within the plane perpendicular to the *c*-axis above the reorientation temperature $T_R = 125$ K but it is off the *c* plane below T_R . Thus, at T_R , the first-order axis-plane spin reorientation phase transition is observed. A mechanism of this transition was discussed by Adachi and Sato⁷ and Adachi.^{8,9} The appearance in the vicinity of T_R of the metamagnetic phase transition related to spin reorientation from the direction perpendicular to the external magnetic field to the direction parallel to the field is an interesting feature of the studied system. Owing to this metamagnetic transition, the Fe₇Se₈ compound is expected to show a large magnetocaloric effect (MCE). Such an effect has not been studied yet in any of the iron-chalcogenide compounds; thus, this paper is devoted to investigating the magnetocaloric effect in a Fe₇Se₈ single crystal and establishing a mechanism responsible for it.

II. EXPERIMENTAL METHODS

The single crystal of nominal composition Fe₇Se₈ was grown by applying Bridgman's method. The sample was prepared from appropriate quantities of Fe lumps (vacuum remelted, low oxygen, 4N, Alfa Aesar) and Se shots (amorphous, Puratronic®, 5N, Alfa Aesar). All the materials were weighted, mixed, and placed into the Bridgman quartz ampoule in an argon filled glove box. A double-wall evacuated (9.32×10^{-5} Pa) and sealed ampoule ($\phi_{in} = 9$ mm) with

starting elements (total mass ~ 3 g) was placed in a furnace with the average vertical gradient of temperature ~ 1.3 °C/mm (maximally up to ~ 2.9 °C/mm—along the first 60 mm). The material was synthesized over ~ 4 h at a temperature up to 680 °C. After melting the ingot at 1075 °C¹⁰ the temperature was held for 6 h, then it was reduced to 350 °C at the rate of 2.0 °C/h, held at this value for 18 h, and then it was lowered down to room temperature at the rate 300 °C/h. The obtained single crystal exhibited well-developed (001) natural surfaces.

The quantitative analysis of the chemical composition was performed on the (110) cleavage plane of the crystal by applying the Energy Dispersive X-ray (EDX) method with the use of the X-MAX Silicon Drift Detector (Oxford Instruments) coupled with the JEOL JSM-7600F field emission (Schottky type) scanning electron microscope (FESEM), operating at 20 kV incident energy.

The orientation of the crystals was determined at room temperature by using the KM-4 KUMA-Diffraction single crystal x-ray diffractometer with the Cu radiation source, the 002 graphite monochromator on the primary beam, the 4-circle kappa goniometer, and the scintillation detector.

The powder x-ray diffraction measurements were carried out on the laboratory Rigaku-Denki D/MAX RAPID II-R diffractometer attached to a rotating anode Ag K α tube ($\lambda = 0.5608$ Å), an incident beam (002) graphite monochromator, and an image plate detector in the Debye-Scherrer geometry. The pixel size was $100\text{ }\mu\text{m} \times 100\text{ }\mu\text{m}$. The powder Fe₇Se₈ sample was placed inside a glass capillary (0.3 mm in diameter). The measurements were performed for the empty capillary and for the capillary filled with the sample. Then, the intensity for the empty capillary was subtracted from the intensity of the filled capillary. The beam width at the sample was 0.1 mm. The two-dimensional diffraction patterns were converted into the one-dimensional intensity data plot. The measurements have been performed within the temperature range from 100 to 500 K using the Cryostream 500 Plus Oxford temperature controller.

Magnetization as a function of temperature and magnetic field was investigated using the commercial superconducting quantum interference device magnetometer (MPMS-7XL SQUID, Quantum Design), within the temperature range 5–490 K and in magnetic field up to 5 T. The experiments have been performed on the oriented, single crystalline Fe₇Se₈ sample that had a shape of a rectangular parallelepiped ($2 \times 2 \times 1.9$ mm³).

Direct measurements of the magnetocaloric effect, i.e., the measurements of adiabatic temperature change (ΔT_{ad}) induced by a change of the external magnetic field, were performed using the Cu-CuNi thermocouple, in the magnetic field varying quickly (6 T/s) from -1.7 to +1.7 T. The experiments were performed for the temperature range 70–370 K.

Specific heat was measured by means of the relaxation method, using the standard HC option of the Physical Property Measurement System (PPMS), made by Quantum Design. Estimated uncertainty of the determined specific heat values was $\sim 2\%$. For $B = 0$, the studies were done in the temperature range from 2 to 300 K.

III. STRUCTURAL AND MAGNETIC PROPERTIES

A. SEM/EDX and single crystal x-ray diffraction

The chemical composition of the crystal has been verified prior to this study. Five points at three areas of the crystal were checked. The average chemical composition of the crystal, determined by SEM/EDX techniques, was equal to Fe_{6.98 \pm 0.13}Se_{8.02 \pm 0.17}.

Based on the single crystal x-ray diffraction measurements, the lattice parameters of the identified 3c-Fe₇Se₈ phase (the trigonal symmetry described by the space group $P3_121$, no. 152) were determined to be equal to $a = 7.245$ Å and $c = 17.67$ Å. Obtained parameters are in good agreement with the previously reported results.^{10–12}

B. Temperature dependent powder x-ray diffraction

The obtained x-ray diffraction results confirmed that the crystal grown was single phase and had the 3c-Fe₇Se₈ structure.^{4,12–14} All the measured diffraction patterns have been gathered in Fig. 1. The further Rietveld refinement analysis has been performed using the FullProf Site software package.¹⁵ All the recorded diffraction peaks have been indexed for the trigonal symmetry with the $P3_121$ space group (number 152), according to the 01-071-0586 record of the PDF-2 database. All the atoms are located in the unit cell in five positions for Fe and four positions for Se atoms. The iron atoms are located in the following Wyckoff positions: Fe1 in $3b$ ($x,0,5/6$), Fe2 and Fe3 in $3a$ ($x,0,1/3$), and Fe4 and Fe5 in $6c$ (x,y,z). All the selenium atoms from Se1 to Se4 are located in $6c$ (x,y,z) positions. All the 1147 recorded peaks have been refined for all the diffraction patterns and the calculated final R_{Bragg} was smaller than 7% for all the refinements. Based on such refinement analysis, the temperature evolution of the lattice constants [Fig. 2(a)], the c/a ratio, and the unit cell volume V [Fig. 2(c)], as well as of the Fe-Fe bond length [Fig. 2(b)] have been plotted.

From the lattice constants analysis [visualized in Fig. 2(a)] it is clearly seen that the $a = b$ parameter increases with increasing temperature in the 100–500 K range, while

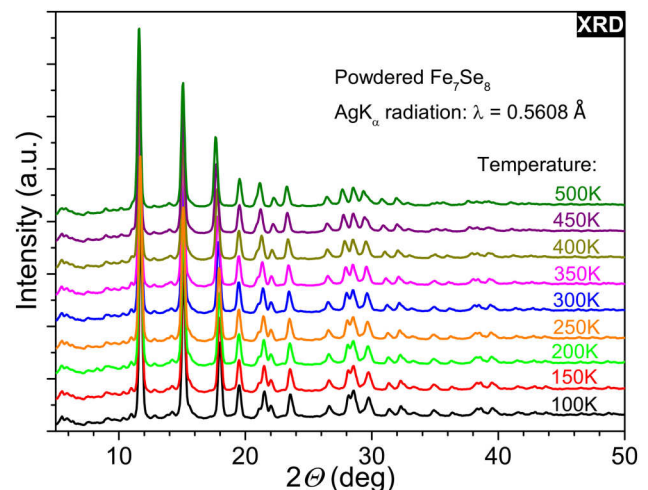


FIG. 1. X-ray diffraction patterns recorded for different temperatures in the range 100–500 K with the step of 50 K.

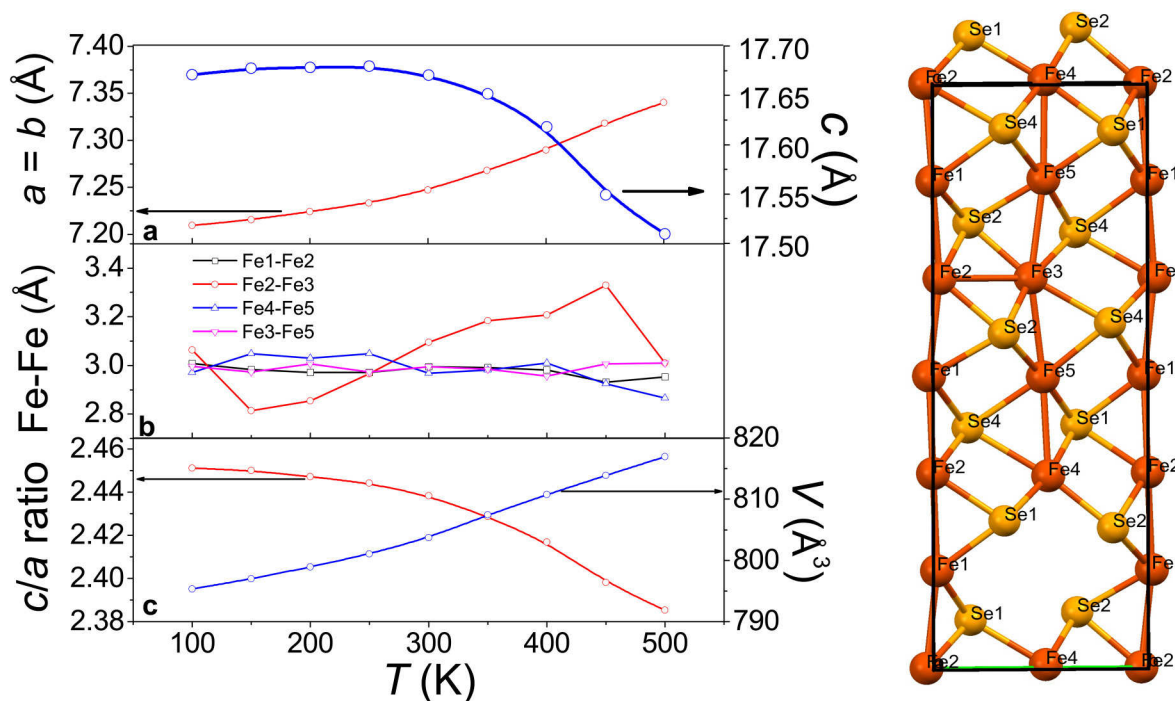


FIG. 2. Structural data of the Fe_7Se_8 crystal. The lattice constants (a), the Fe-Fe bond lengths (b), and the c/a ratio and the unit cell volume (c) as a function of temperature were determined from the Rietveld refinement analysis. The right panel presents the arrangement of atoms in the unit cell in the yz plane for $x \approx 0$. The vacancies are located along the c -axis in such a way that continuous $-Fe1-Fe2-$ chains and the chains consisting of five atom segments $Fe4-Fe5-Fe3-Fe5-Fe4$ separated by vacancies can be distinguished.

the c parameter has almost a constant value of 17.67–17.68 Å in the temperature range from 100 up to 250 K, and then it decreases strongly from 17.68 Å at 250 K down to 17.52 Å at 500 K. The monotonous decrease of the c/a ratio and increase of the unit cell volume [Fig. 2(c)] with increasing temperature prove that the effect of elongation in the x - y plane is more pronounced than the contraction in the z -direction. To analyze the structure evolution as a function of temperature in more detail, the analysis of the Fe-Fe bond length has been performed and the obtained results are plotted in Fig. 2(b). From the analysis of this figure, it is clearly seen that the Fe-Fe distances in the infinite continuous chains $-Fe1-Fe2-$ and in the five atomic chain segments $Fe4-Fe5-Fe3-Fe5-Fe4$ decrease with increasing temperature, while the Fe2-Fe3 bond length reaches a minimum value of 2.8 Å at 150 K and then increases to a maximum value of 3.3 Å at 450 K.

Additionally, strong changes in the Fe2-Fe3 distance could be correlated with the magnetic transitions, since the minimum distance of 2.8 Å at 150 K was measured close to the first order phase transition, while the maximum distance of 3.3 Å was measured at 450 K, i.e., close to the second order phase transition temperature, T_N .

C. Magnetic measurements

Figure 3(a) shows the temperature dependence of magnetization, M , in low magnetic field $B = 0.01$ T oriented parallel to the c -axis. The $M(T)$ dependence indicates that the reorientation of spins from the easy magnetization c -axis to the easy plane perpendicular to the c -axis appears at the temperature of about 125 K. The estimated

reorientation temperature agrees with the literature data.¹⁶ According to the neutron investigations performed by Kawaminami and Okazaki,³ as well as by Andresen and Leciejewicz,¹⁷ the magnetic ordering of $3c$ - Fe_7Se_8 is a ferrimagnetic one.

The sharp change of $M(T)$ at the spin-reorientation phase transition and the difference between the field-cooled (FC) magnetization values measured during cooling (FCC) and warming (FCW) cycles indicate the first order character of this transition. In the magnetic field parallel to the c -axis [Fig. 3(a)], the magnetization is close to zero at temperatures higher than the temperature of spin reorientation. It means that on warming, at the temperature of about 125 K, there is transition from the ferrimagnetic phase with the moments directed along the c -axis to the phase in which magnetic moments are directed nearly perpendicularly to the c -axis.

Figure 3(b) presents the temperature dependence of magnetization in magnetic field $B = 0.01$ T perpendicular to the c -axis of the Fe_7Se_8 single crystal. In accordance with the scenario presented above, very low magnetic moment is observed below the first order phase transition temperature. The rapid increase of magnetization with increasing temperature at the spin reorientation temperature is the result of nearly perpendicular alignment of the spins to the c -axis.

The effect of increase of the transition temperature with an increase of the magnetic field parallel to the c -axis has been observed [Fig. 3(c)]. For magnetic field applied perpendicularly to the c -axis, [Fig. 3(d)], the behavior of magnetization opposite to that appearing in $B \parallel c$ was

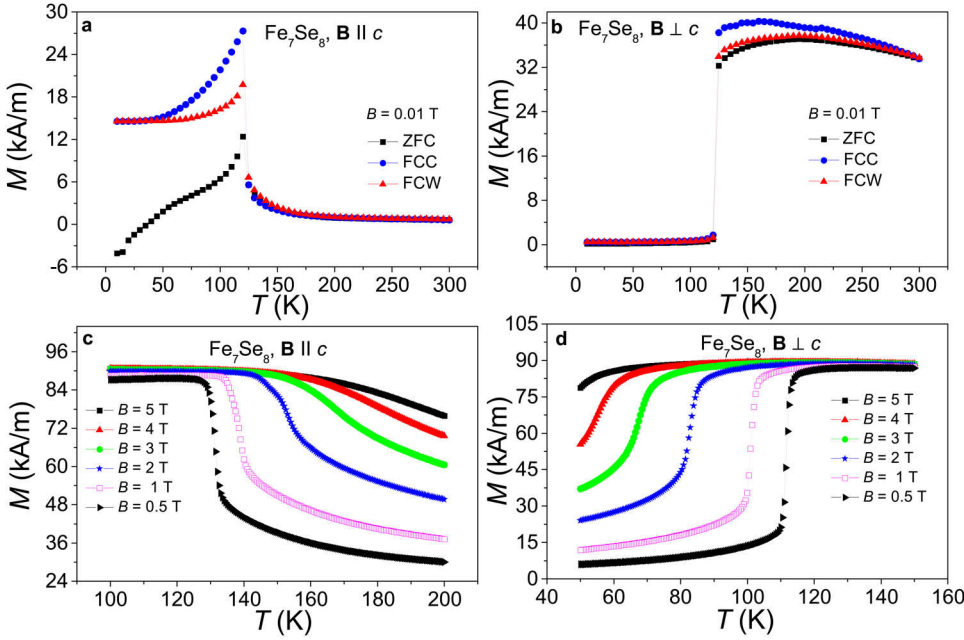


FIG. 3. Magnetization as a function of temperature. (a) and (b) Dependences measured in magnetic field $B = 0.01$ T directed, respectively, parallel and perpendicularly to the crystallographic c -axis of the Fe_7Se_8 single crystal. (c) and (d) The same dependences for fixed B values ranging from 0.5 to 5 T, and the field oriented, respectively, parallel and perpendicularly to the c -axis. Abbreviations ZFC, FCC, and FCW denote, respectively, measurements in the field on warming the sample cooled previously in zero field, measurements in the field on cooling the sample, and measurements in the field on warming the sample cooled previously in the same field. For $B \geq 0.5$ T, there are no differences between the ZFC, FC, and FCW cycles.

observed. In the case of $\mathbf{B} \perp c$, the transition temperature from the phase with spin ordering along the applied magnetic field decreases with increasing magnetic field because of the Zeeman energy.

D. Metamagnetic phase transitions in Fe_7Se_8 single crystal

Field dependence of magnetization at constant temperature, $T = 10$ K, for magnetic field applied parallel and perpendicularly to the c -axis is presented in Fig. 4(a). For $\mathbf{B} \parallel c$, the saturation of magnetization is observed in relatively low magnetic field $B \approx 0.35$ T. In the field directed perpendicularly to the c -axis, the saturation of magnetization was not observed even in high magnetic field $B = 5$ T. Such kind of magnetic behavior indicates the strong uniaxial magnetic anisotropy of the Fe_7Se_8 single crystal with the easy magnetization direction parallel to the c -axis.

A rapid increase of magnetization of the $3c\text{-Fe}_7\text{Se}_8$ crystal with an increase of magnetic field was observed for the first time by Kamimura¹⁸ for temperatures close to the spin reorientation temperature. The magnetization measured in the magnetic field parallel to the c -axis at a temperature higher than the reorientation temperature is typical of a material showing a metamagnetic transition [Fig. 4(b)]. For such kind of transition, magnetization curves have a specific, so called S-like, shape.^{16,19} The similar metamagnetic transition was observed also [Fig. 4(c)] in magnetization curves measured in magnetic field applied perpendicularly to the c -axis at temperatures lower than the spin reorientation temperature of the Fe_7Se_8 single crystals.

E. Magnetic behavior near the Néel temperature

Figure 5 shows the temperature dependences of magnetization measured for a series of fixed values of the magnetic field directed perpendicularly to the c -axis, in order to calculate the value of the magnetocaloric effect near the second

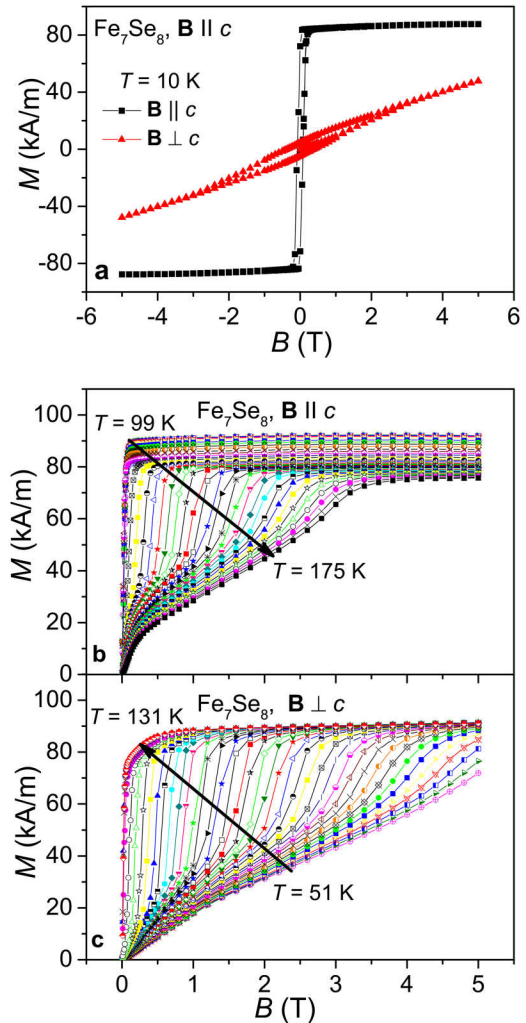


FIG. 4. Magnetization as a function of magnetic field parallel [panels (a) and (b)] and perpendicular [panels (a) and (c)] to the c -axis: (a) at the temperature of 10 K, and (b) and (c) at fixed temperatures ranging with the step of 2 K from 99 to 175 K [panel (b)] and from 51 to 131 K [panel (c)].

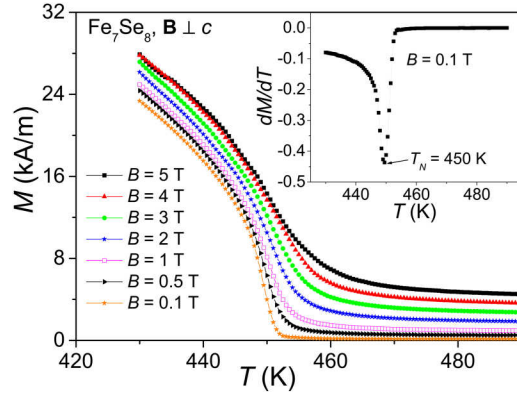


FIG. 5. Temperature dependences of magnetization at magnetic field oriented perpendicularly to the crystallographic c -axis of the Fe_7Se_8 single crystal, recorded in the vicinity of the Néel temperature. The inset presents temperature dependence of dM/dT at the magnetic field $B = 0.1$ T applied along the same direction.

order phase transition from the ferrimagnetic phase to the paramagnetic phase. These dependences are typical of the material showing the second order transition. The Néel temperature, assumed to be equal to the temperature at which dM/dT [inset to Fig. (5)] reaches a minimum, was estimated to be $T_N \approx 450$ K. This value is close to the literature data $T_N \approx 455.3$ K.³

IV. MAGNETOCALORIC EFFECT IN THE Fe_7Se_8 SINGLE CRYSTAL

A. Calculations based on the Maxwell relation

The results of isothermal and isofield measurements of magnetization have been used in order to calculate the isothermal magnetic entropy change, based on the Maxwell relation [Eq. (17) in Ref. 20],

$$\Delta S(T, H) = \int_0^H \left(\frac{\partial M}{\partial T} \right)_H dH. \quad (1)$$

In this paper, the integration appearing in (1) was performed by using the trapezoidal method.²¹ In order to assess roughly a performance of the considered material for refrigeration, we calculated two commonly used parameters the “Refrigeration Capacity,” RC,

$$RC = \int_{T_1}^{T_2} \Delta S(T) dT, \quad (2)$$

where T_1 and T_2 are the temperatures corresponding to the full width at half maximum of $-\Delta S$ and the “Temperature Averaged Entropy Change,” given by the following formula [Eq. (11) in Ref. 22]:

$$TEC(\Delta T_{\text{lift}}, \Delta B) = \frac{1}{\Delta T_{\text{lift}}} \max_{T_{\text{mid}}} \left[\int_{T_{\text{mid}} - \frac{T_{\text{lift}}}{2}}^{T_{\text{mid}} + \frac{T_{\text{lift}}}{2}} \Delta S(T)_{\Delta B} dT \right], \quad (3)$$

where ΔT_{lift} denotes the expected temperature change in response to the change of the external magnetic field, ΔB . The calculations were performed assuming $\Delta B = 2$ T and $\Delta T_{\text{lift}} = 3$ and 10 K, i.e., the values often considered in the literature.²²

The magnetic entropy change calculated based on the Maxwell relation reveals the presence of the normal, i.e., related to decrease of entropy with an increase of the applied field, magnetocaloric effect (MCE) in the magnetic field applied parallel to the crystallographic c -axis of the Fe_7Se_8 crystal [Fig. 6(a)]. This MCE is related to the first order phase transition from the low temperature “parallel to c ” phase to the high temperature “perpendicular to c ” phase, i.e., easy axis-easy plane transition, appearing near 125 K. The magnetic entropy change peaks expand to higher temperatures with an increase in intensity of the external magnetic field applied parallel to the c -axis [Fig. 6(a)]. The expansion of the ΔS peak to higher temperatures, visible in Fig. 6(a), is due to the shift of the metamagnetic transition towards higher temperatures under the influence of the strong external magnetic field [see Figs. 3(a), 3(c), 4(a), and 4(b)]. For the change of the magnetic field parallel to the c -axis from 0 to 2 T, the maximum magnetic entropy change is equal to $|\Delta S_m| \approx 0.54$ J/(kg K), the refrigeration capacity calculated according to Eq. (2) is equal to $|RC| \approx 19.7$ J/kg (for $T_1 = 99$ K and $T_2 = 175$ K), and $|TEC(3 \text{ K}, 2 \text{ T})| \approx |TEC(10 \text{ K}, 2 \text{ T})| \approx 0.30$ J/(kg K).

The temperature dependences of magnetic entropy change, presented in Fig. 6(b), reflect the so-called inverse magnetocaloric effect, i.e., the effect in which entropy of a system increases with an increase of an external magnetic field, appearing in the magnetic field applied perpendicularly to the c -axis. In this case, the expansion of magnetic entropy change towards low temperatures in high magnetic field is also related to the metamagnetic transition. The maximal magnetic entropy change is equal to $\Delta S \approx 0.53$ J/(kg K) in the vicinity of the first order phase transition in the magnetic field $B = 2$ T and the corresponding refrigeration capacity is equal to $|RC| \approx 22$ J/kg (the integration was performed over the temperature range from 51 to 131 K), $TEC(3 \text{ K}, 2 \text{ T}) \approx 0.29$ J/(kg K), and $TEC(10 \text{ K}, 2 \text{ T}) \approx 0.39$ J/(kg K).

The $M(T)$ data presented in Fig. 5 were used to calculate the temperature dependence of the magnetic entropy change in the magnetic field perpendicular to the crystallographic c -axis, near the second order phase transition occurring at T_N .

The magnetic entropy change as a function of temperature is shown in Fig. 6(c). Such a shape of the $\Delta S(T)$ dependences is typical of the second order phase transition from the ferrimagnetic to the paramagnetic phase. The maximum magnetic entropy change is equal to $\Delta S \approx -0.60$ J/(kg K) near $T_N \approx 450$ K in the magnetic field $B = 2$ T. The maximum ΔS value near the second order phase transition is about 12% larger than the maximum magnetocaloric effect in the vicinity of the first order phase transition. The corresponding refrigeration capacity is equal to $|RC| \approx 4.2$ J/kg, in the magnetic field $B = 2$ T, $|TEC(3 \text{ K}, 2 \text{ T})| \approx 0.33$ J/(kg K), and $|TEC(10 \text{ K}, 2 \text{ T})| \approx 0.29$ J/(kg K). The determined $|RC|$ is five times lower in comparison with the value obtained near the first order phase transition temperature.

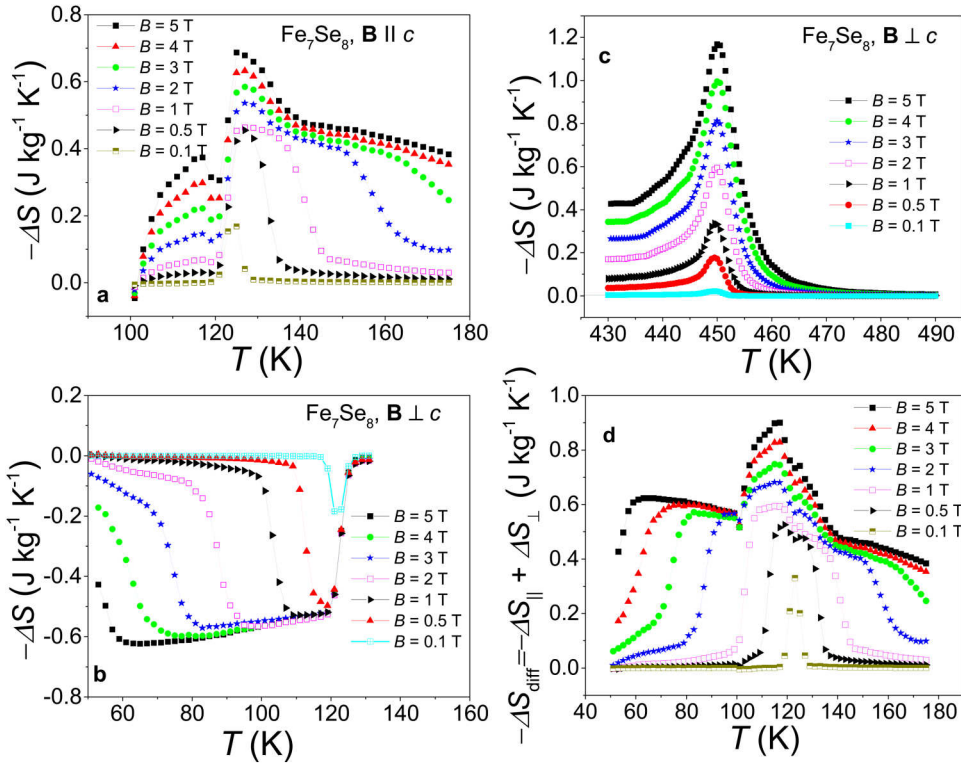


FIG. 6. Temperature dependence of magnetic entropy change in magnetic field applied parallelly (a) and perpendicularly (b), (c) to the c -axis. Panels (a) and (b) present the data obtained at low temperature in the vicinity of the metamagnetic transition, while high temperature data recorded in the vicinity of the Néel temperature are presented in panel (c). Panel (d) presents the difference between the magnetic entropy changes in magnetic field applied parallelly and perpendicularly to the c -axis.

The difference between the magnetic entropy change in the magnetic field parallel and in the field perpendicular to the c -axis is presented in Fig. 6(d). The broad magnetic entropy change peak of rotational MCE shows the very wide working temperature range of about 60 K in the magnetic field $B = 2$ T and it increases with increasing external magnetic field, which is potentially perspective for application. Unfortunately, the rotational MCE (ΔS_{diff}) of Fe_7Se_8 of about $\Delta S_{\text{diff}} = 0.7 \text{ J/(kg K)}$ is lower in comparison with the literature data for other materials²³ with $\Delta S_{\text{diff}} = 11.1 \text{ J/(kg K)}$ in the magnetic field $B = 2$ T. Nevertheless, it should be stressed that in Fe_7Se_8 crystals, in the vicinity of the spin reorientation transition, the rotating MCE is larger than the non-rotational one. This result is in contrast with Ref. 23 and it is one of the most interesting features of Fe_7Se_8 .

B. Direct measurement of magnetocaloric effect

The adiabatic temperature change (ΔT_{ad}) of the Fe_7Se_8 single crystal under the influence of magnetic field was also measured directly. Figure 7 presents the temperature dependence of ΔT_{ad} for the magnetic field perpendicular to the c -axis, increasing from 0 to 1.7 T. For this geometry, the presented dependence shows negative ΔT_{ad} values, characteristic of the, so called, inverse magnetocaloric effect. This behavior agrees with the results of the indirect measurements. The extremal ΔT_{ad} was observed at the temperature near 86 K, which means that the maximum of adiabatic temperature change is shifted to the lower temperature in comparison with the temperature of the first order phase transition, equal approximately to 125 K in low magnetic field. This effect can be attributed to the fact, clearly seen in the measured $M(T, H)$ dependences [Fig. 3(d)], that the first order phase

transition temperature decreases with an increase of the external magnetic field.

C. Calculations of the magnetocaloric effect based on the heat capacity measurements

For $B = 0$, specific heat of the Fe_7Se_8 single crystal was measured from 2 to 300 K. Since no phase transitions appeared within the range 122–300 K, for nonzero B values, ranging from 1 up to 5 T, the specific heat was measured up to 200 K only (the magnetic field B was applied both along and perpendicular to the c -axis). The experimental points were recorded with the step of 0.2 K within temperature regions close to the phase transitions.

The temperature dependences of heat capacity in magnetic field applied perpendicularly to the c -axis are presented in Fig. 8(a). For zero magnetic field, the heat capacity reaches a maximum, related to the first order spin

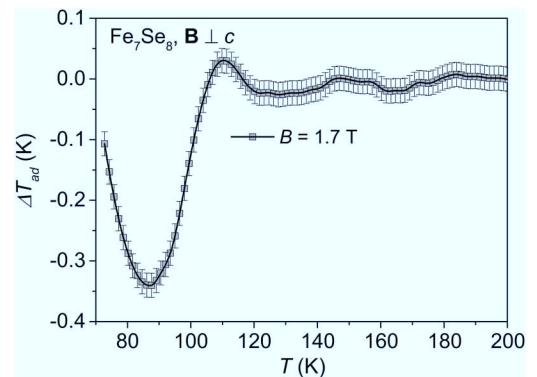


FIG. 7. Temperature dependence of the adiabatic temperature change for the magnetic field of 1.7 T applied perpendicularly to the c -axis.

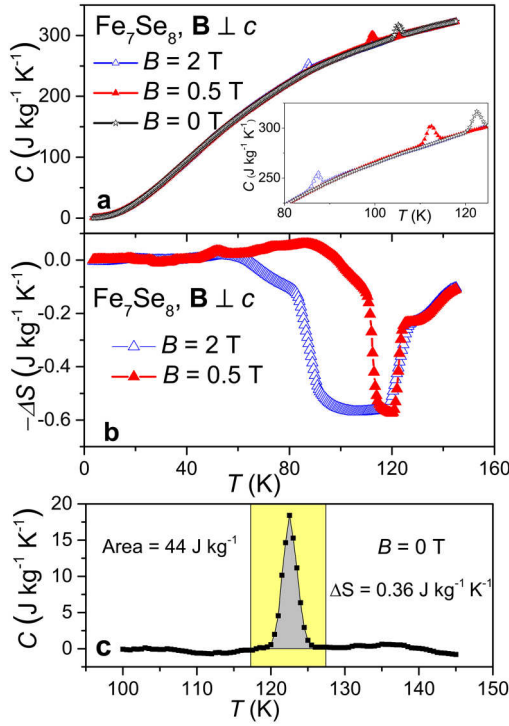


FIG. 8. (a) Temperature dependences of the heat capacity measured in magnetic field applied perpendicularly to the c -axis. (b) Calculated temperature dependences of the isothermal change of entropy, appearing as a result of an increase of the magnetic field from 0 to 0.5 T and from 0 to 2 T. (c) Area below the anomaly related to the spin-reorientation transition, approximately equal to the latent heat of the transition.

reorientation phase transition, at the temperature close to 123 K. The shift of this maximum under the influence of the magnetic field is in agreement with the shift of the transition temperature visible in Fig. 3(d).

The entropy is defined by the following formula:

$$S_B(T) = \int_0^T \frac{C_B(T)}{T} dT + S_B(0), \quad (4)$$

where $C_B(T)$ denotes the temperature dependence of specific heat measured at a fixed B value. In the calculations, it was assumed that $S_B(0) = 0$ independently of the B value. Then, the $\Delta S_B(T)$ dependences were calculated as

$$\Delta S(T, B) = S_B(T) - S_0(T). \quad (5)$$

The results are presented in Fig. 8(b).

As it can be seen from Fig. 8(b), the maximum of the magnetic entropy change broadens with an increase of the final external magnetic field value. The temperature dependences of the magnetic entropy change calculated based on the heat capacity measurements are in fair agreement with those calculated based on the magnetization measurements, Fig. 6(b). In particular, for the magnetic field directed perpendicularly to the c -axis, for 119 K, the values calculated based on the specific heat data are larger by ca. 13% for the final field of 0.5 T and by ca. 4% for the final field of 2 T, than those calculated based on the magnetization data.

After subtracting the lattice contribution to the specific heat, the area below the specific heat anomaly related to the

spin-reorientation transition, which should be approximately equal to the latent heat of the 1st order transition, was calculated. The equality mentioned above is approximate only, because in the case of the 1st order transition the anomaly is very sharp, resembling the delta function, and the relaxation method of measurement, which was applied in the present studies, and which consists in supplying small measuring heating pulses increasing temperature of the sample, smears the anomaly and disturbs its shape. This is the well known imperfection of the relaxation method. Then, by using the equation

$$Q_L = \Delta S_m T_R, \quad (6)$$

the entropy jump at the transition, $\Delta S_m = 0.38(3)$ J/(kg K), was determined for $B = 0, 2$, and 5 T.

Finally, the temperature dependences of the adiabatic temperature change induced by applying the external field, Fig. 9, were assessed by using the following approximate relation given in Refs. 24 and 25:

$$\Delta T = -\frac{T \Delta S}{C}. \quad (7)$$

D. Theoretical estimation of magnetocaloric effect

A free energy per unit mass of Fe₇Se₈ can be expressed as follows:¹⁶

$$E(\theta) = -P k_B T \ln \sum_i \exp[-\varepsilon_i(\theta)/k_B T] + K_1 \cos^2 \theta - H M_s \cos(\theta - \theta_H). \quad (8)$$

The first term describes the single ion anisotropy of the ferrous ions, the second term comes from dipole-dipole interactions between all iron ions, and the third term is the

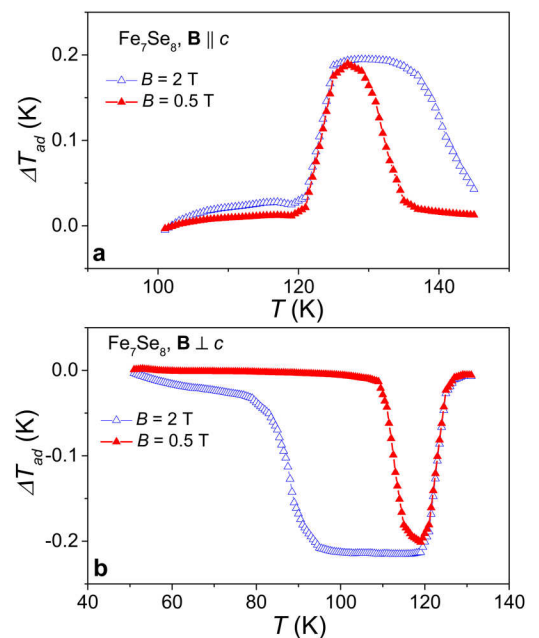


FIG. 9. Temperature dependence of the adiabatic temperature change induced by the magnetic field applied along (a) and perpendicularly to (b) the c -axis, calculated according to Eq. (7).

Zeeman interaction. In Eq. (8), the ε_i are the triplet energy levels of the ferrous ion, the coefficient P is proportional to the fraction of the ferrous ions in the lowest degenerate orbital state. The values of ε_i are the solutions of cubic equation [Eq. (1) in Ref. 16],

$$\varepsilon^3 - \varepsilon_i \varepsilon^2 - \eta^2 [(l_z^2 - l_z - 2) \cos^2 \theta + (l_z + 2)] \varepsilon + \eta^2 l_z^2 \varepsilon_i \cos^2 \theta = 0, \quad (9)$$

where θ is the angle of the spin direction in the z axis, l_z is the z component of the orbital angular momentum in the degenerate orbital state, and ε_i is the energy splitting due to the trigonal field, $\eta = \lambda S$. In the calculation of the triplet levels, the following values of the parameters appearing in Eq. (9) were assumed: $l_z = -0.55$, $\eta/k_B = 253$ K, and $\varepsilon_i/k_B = 760$ K.

Using Eq. (9), it is possible to simulate the magnetic entropy change in the applied magnetic field,

$$-\Delta S = -[S(T, B) - S(T, 0)] = \frac{\partial E(T, B)}{\partial T} - \frac{\partial E(T, 0)}{\partial T}. \quad (10)$$

The results of simulations for magnetic field applied along and perpendicular to the c -axis are shown in Figs. 10(a) and 10(b), respectively.

The good agreement with the experiment was achieved for $Pk_B = 24$ J/(kg K), $K_1 = 53$ J/kg, and $M_s = 14.5$ A m²/kg. The parameter Pk_B corresponds to approximately $\sim 43\%$ of ferrous (Fe^{2+}) atoms' fraction, which is of the same order of magnitude as the expected 5/7 percentage value.

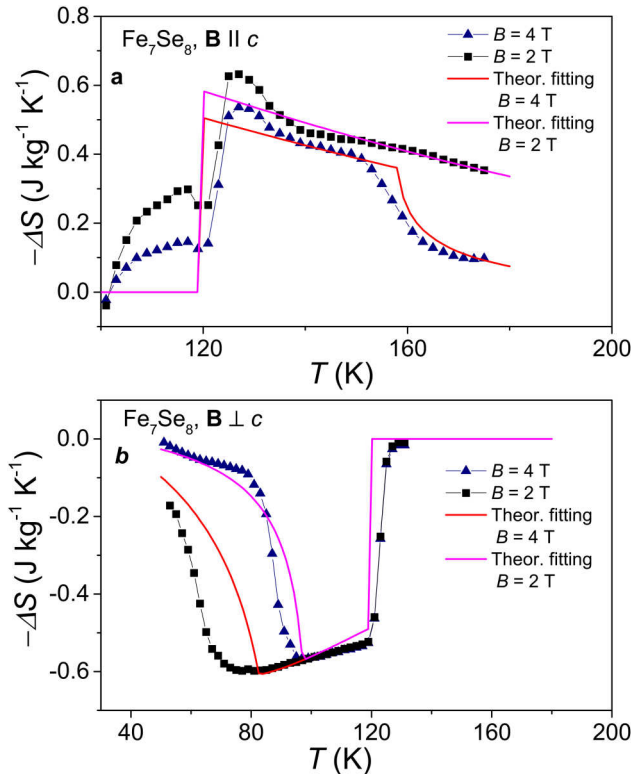


FIG. 10. Fitting of the theoretical temperature dependences of the magnetic entropy change in the magnetic field parallel (a) and perpendicular (b) to the c -axis to the experimental data.

The performed simulation confirms the single ion mechanism to be responsible for the magnetocaloric effect in Fe_7Se_8 single crystals.

V. SUMMARY AND CONCLUSIONS

The Fe_7Se_8 single crystals have been grown by applying Bridgman's method. Magnetization, magnetocaloric, and calorimetric measurements have been carried out in a magnetic field up to 5 T over the temperature range from 5 to 490 K. The reorientation spin transition from the easy c -axis to the easy plane perpendicular to the c -axis state has been observed near the temperature $T_R \approx 125$ K. It proceeds abruptly, as the first-order phase transition. The magnetization curves in the vicinity of this transition were measured and the influence of the external magnetic field on the transition point was studied. The magnetic field directed along the c -axis was found to shift the metamagnetic transition towards temperatures higher than T_R , whereas the field directed perpendicularly to the c -axis was found to shift the transition towards temperatures lower than T_R . Thus, the conventional magnetocaloric effect related to the metamagnetic transitions has been found above T_R , in the magnetic field parallel to the c -axis, while the inverse magnetocaloric effect was observed below T_R , in the field perpendicular to the c -axis. The existence of both kinds of magnetocaloric effect is important from the point of view of a large entropy change in the rotating field in the Fe_7Se_8 single crystal. The second order phase transition to the paramagnetic state has been studied at the Néel temperature $T_N = 450$ K. The maximum value of the isothermal entropy change associated with this transition is larger than the one observed near T_R . However, the refrigeration capacity related to the transition at T_N is smaller than that related to the spin reorientation transition. The one-ion model of the magnetocaloric effect, based on the considerations presented in Ref. 16, has been developed and fair agreement between the results of calculations performed within it and the experimental data was found.

In the presented studies, the results of application of three methods of analysis of the magnetocaloric effect, i.e., of the Maxwell relation, direct measurement, and specific heat measurement methods were compared. As it was analyzed wider, e.g., in Ref. 26 each of them has its own advantages and drawbacks. In particular, the "Maxwell relation method" allows us to determine the isothermal entropy change quickly and accurately; however, gives no information on the adiabatic temperature change and fails in the vicinity of some sharp, 1st order phase transition, where abrupt magnetization change appears and accurate calculation of its temperature derivative is impossible. The "direct measurement method" allows us to determine the adiabatic temperature change; however, it gives no information on the entropy change. Its accuracy can be negatively influenced by the heat capacity of the sample holder and a temperature sensor, as well as by the impact of the magnetic field applied on indications of the thermometer. The latter issue is particularly important because thermocouples, often used in this method due to their low heat capacity, are very sensitive to the field. The "heat capacity" method seems to be the most

universal, as the method allows us to calculate the $S(T, B)$ dependences and to determine both the isothermal entropy change, Eq. (5), and the adiabatic temperature change, by solving the equation $S(T + \Delta T_{\text{ad}}, B) = S(T, 0)$. However, the entropy of the system got by the integration (4) is usually a large quantity, whereas we are interested in the small difference between the two large entropy values determined for different B . As a result, the determined values of both parameters bear rather large experimental uncertainty. It should be mentioned that also the fourth method, the usage of the Clausius-Clapeyron equation, is often used in analysis of the magnetocaloric effect. This method supplies information on the contribution to the isothermal change of entropy coming from the latent heat of a 1st order transition, i.e., from the change of entropy related to the 1st order transition. However, this method gives no information on the change in entropy that appears in the system “normally”, before reaching the phase transition point. Thus, it is a complementary method to the “Maxwell relation”, and allows us to determine the entropy change at the points at which the latter method fails.

In conclusion, the determined $|\Delta S| \sim 0.6 \text{ J/(kg K)}$ and $|\Delta T_{\text{ad}}| \sim 0.3 \text{ K}$ values for $B \approx 2 \text{ T}$ do not place the Fe_7Se_8 crystals among materials especially attractive for applications. Nevertheless, due to the large anisotropy and the presence of the spin-reorientation transition, which are the origins of the considerable magnetocaloric effect, Fe_7Se_8 seems to be attractive as the model material in considerations of the devices based on rotation of the active magnetocaloric medium in the magnetic field, not on inserting and extracting the medium from the field.

ACKNOWLEDGMENTS

This study was partly financed by the National Centre for Research and Development, Research Project No. PBS2/A5/36/2013, the National Science Centre of Poland based on Decision No. DEC-2013/08/M/ST3/00927, and the European Union, within the European Regional Development

Fund, through the Innovative Economy Grant No. POIG.01.01.02-00-108/09.

- ¹F. C. Hsu, J. Y. Luo, K. W. Yeh, T. K. Chen, T. W. Huang, P. M. Wu, Y. C. Lee, Y. L. Huang, Y. Y. Chu, D. C. Yan, and M. K. Wu, *Proc. Natl. Acad. Sci. U.S.A.* **38**, 14262 (2008).
- ²G. W. Li, B. M. Zhang, T. Baluyan, J. C. Rao, J. Q. Wu, A. A. Novakova, P. Rudolf, G. R. Blake, R. A. de Groot, and T. T. M. Palstra, *Inorg. Chem.* **55**, 12912 (2016).
- ³M. Kawaminami and A. Okazaki, *J. Phys. Soc. Jpn.* **29**, 649 (1970).
- ⁴A. Okazaki and K. Hirakawa, *J. Phys. Soc. Jpn.* **11**, 930 (1956).
- ⁵A. Okazaki, *J. Phys. Soc. Jpn.* **16**, 1162 (1961).
- ⁶M. E. Fleet, *Acta Cryst. B* **27**, 1864 (1971).
- ⁷K. Adachi and K. Sato, *J. Appl. Phys.* **39**, 1343 (1968).
- ⁸K. Adachi, *J. Phys. Soc. Jpn.* **16**, 2187 (1961).
- ⁹K. Adachi, *J. Phys. France* **24**, 725 (1963).
- ¹⁰H. Okamoto, *J. Phase Equilib.* **12**, 383 (1991).
- ¹¹L. Calvert, *National Research Council of Canada* (ICDD Grant-in-Aid, Ottawa, Canada, 1980).
- ¹²J. B. Parise, A. Nakano, M. Tokonami, and N. Morimoto, *Acta Cryst. B* **35**, 1210 (1979).
- ¹³A. Okazaki, *J. Phys. Soc. Jpn.* **14**, 112 (1959).
- ¹⁴H. N. Ok, K. S. Baek, and E. C. Kim, *Solid State Commun.* **87**, 1169 (1993).
- ¹⁵J. Rodríguez-Carvajal, *Physica B* **192**, 55 (1993).
- ¹⁶T. Kamimura, *J. Phys. Soc. Jpn.* **43**, 1594 (1977).
- ¹⁷A. F. Andresen and J. Leciejewicz, *J. de Physique* **25**, 574 (1964).
- ¹⁸T. Kamimura, *J. Phys. Soc. Jpn.* **51**, 80 (1982).
- ¹⁹E. Strykowski and N. Giordano, *Adv. Phys.* **26**, 487 (1977).
- ²⁰A. Smith, C. R. H. Bahl, R. Björk, K. Engelbrecht, K. K. Nielsen, and N. Pryds, *Adv. Energy Mater.* **2**, 1288 (2012).
- ²¹W. H. Press, S. A. Teukolsky, W. T. Vetterling, and B. P. Flannery, *Numerical Recipes, The Art of Scientific Computing*, 3rd ed. (Cambridge University Press, Cambridge, 2007).
- ²²L. D. Griffith, Y. Mudryk, J. Slaughter, and V. K. Pecharsky, *J. Appl. Phys.* **123**, 034902 (2018).
- ²³Hu Zhang, YaWei Li, Enke Liu, YaJiao Ke, JinLing Jin, Yi Long, and BaoGen Shen, *Sci. Rep.* **5**, 11929 (2015).
- ²⁴A. Giguère, M. Foldeaki, B. Ravi Gopal, R. Chahine, T. K. Bose, A. Frydman, and J. A. Barclay, *Phys. Rev. Lett.* **83**, 2262 (1999).
- ²⁵R. Szymczak, N. Nedelko, S. Lewińska, E. Zubov, A. Sivachenko, I. Gribanov, A. Sazanovich, I. Radelytskyi, K. Dyakonov, A. Slawska-Waniewska, V. Valkov, V. Varyukhin, V. Dyakonov, and H. Szymczak, *Solid State Sci.* **36**, 29 (2014).
- ²⁶A. Szewczyk, M. Gutowska, K. Piotrowski, and B. Dabrowski, *J. Appl. Phys.* **94**, 1873 (2003).